

Optical transport and sensing in plexcitonic nanocavities

Olalla Pérez-González,^{1,2} Javier Aizpurua,² and Nerea Zabala^{1,2,*}

¹Department of Electricity and Electronics, University of the Basque Country (UPV/EHU), 48080 Bilbao, Spain

²Material Physics Center CSIC-UPV/EHU and Donostia International Physics Center (DIPC), Paseo Manuel Lardizabal 4, 20018 Donostia-San Sebastián, Spain

*nerea.zabala@ehu.es

Abstract: We present a theoretical study of the optical properties of a strongly coupled metallic dimer when an ensemble of molecules is placed in the inter-particle cavity. The linking molecules are characterized by an excitonic transition which couples to the Bonding Dimer Plasmon (BDP) and the Bonding Quadrupolar Plasmon (BQP) resonances, arising from the hybridization of the dipolar and quadrupolar modes of the individual nanoparticles, respectively. As a consequence, both modes split into two coupled plasmon-exciton modes, so called plexcitons. The Charge Transfer Plasmon (CTP) resonance, involving plasmonic oscillations of the dimer as a whole, arises when the conductance of the excitonic junction is above a threshold value. The possibility of exploiting plexcitonic resonances for sensing is explored in detail. We find high sensitivity to the environment when different dielectric embedding media are considered. Contrary to standard methods, we propose a new framework for effective sensing based on the relative intensity of plexcitonic peaks.

© 2013 Optical Society of America

OCIS codes: (250.0250) Optoelectronics; (250.5403) Plasmonics; (280.4788) Optical sensing and sensors.

References and links

1. M. Pelton, J. Aizpurua, and G. W. Bryant, "Metal-nanoparticle plasmonics," *Laser & Photon. Rev.* **2**, 136–159 (2008).
2. S. Lal, S. Link, and N. J. Halas, "Nano-optics from sensing to waveguiding," *Nat. Photonics* **1**, 641–648 (2007).
3. N.J. Halas, S. Lal, W.S. Chang, S. Link and P. Nordlander, "Plasmons in strongly coupled metallic nanostructures," *Chem. Rev.* **111**, 3913–3961 (2011).
4. A. D. McFarland and R. P. Van Duyne, "Single silver nanoparticles as real-time optical sensors with Zeptomole sensitivity," *Nano Lett.* **3**, 1057–1062, (2003).
5. H. Xu, J. Aizpurua, M. Käll, and P. Apell, "Electromagnetic contributions to single-molecule sensitivity in surface-enhanced Raman scattering," *Phys. Rev. E* **62**, 4318–4324 (2000).
6. M. R. Choi, K. J. Stanton-Maxey, J. K. Stanley, C. S. Levin, R. Bardhan, D. Akin, S. Badve, J. Sturgis, J. P. Robinson, R. Bashir, N. J. Halas, and S.E. Clare, "A cellular Trojan horse for delivery of therapeutic nanoparticles into tumors," *Nano Lett.* **7**, 3759–3765 (2007).
7. H. Atwater and A. Polman, "Plasmonics for improved photovoltaic devices," *Nat. Materials* **9**, 205–213 (2010).
8. Y. B. Zheng, Y. Yang, L. Jensen, L. Fang, B. K. Juluri, A. H. Flood, P. S. Weiss, J. F. Stoddart, and T. J. Huang, "Active molecular plasmonics: controlling plasmon resonances with molecular switches," *Nano Lett.* **9**, 819–825 (2009).
9. J. Aizpurua, P. Hanarp, D. S. Sutherland, M. Käll, G. W. Bryant, and F. J. García de Abajo, "Optical properties of gold nanorings," *Phys. Rev. Lett.* **90**, 057401 (2003).
10. H. Wei, A. Reyes-Coronado, P. Nordlander, J. Aizpurua, and H. Xu, "Multipolar plasmon resonances in individual Ag nanorice," *ACS Nano* **4**, 2649–2654 (2010).

11. C. L. Nehl, H. Liao, and J. H. Hafner, "Optical properties of star-shaped gold nanoparticles," *Nano Lett.* **6**, 683–688 (2006).
12. P. Nordlander, C. Oubre, E. Prodan, K. Li and M. I. Stockman, "Plasmon hybridization in nanoparticle dimers," *Nano Lett.* **4**, 899-903 (2004).
13. T. Atay, J. H. Song, and A. V. Nurmikko, "Strongly interacting plasmon nanoparticle pairs: from dipole-dipole interaction to conductively coupled regime," *Nano Lett.* **4**, 1627–1631 (2004).
14. I. Romero, J. Aizpurua, F. J. García de Abajo and G. W. Bryant, "Plasmons in nearly touching metallic nanoparticles: singular response in the limit of touching dimers," *Opt. Express* **14**, 9988-9999 (2006).
15. J. B. Lassiter, J. Aizpurua, L. I. Hernández, D. W. Brandl, I. Romero, S. Lal, J. H. Hafner, P. Nordlander, and N. J. Halas, "Close encounters between two nanoshells," *Nano Lett.* **8**, 1212–1218 (2008).
16. M. Schnell, A. García-Etxarri, A. Huber, K. Crozier, J. Aizpurua, and R. Hillenbrand, "Controlling the near-field oscillations of loaded plasmonic nanoantennas," *Nat. Photonics* **3**, 287–291 (2009).
17. O. Pérez-González, N. Zabala, A. Borisov, N.J. Halas, P. Nordlander and J. Aizpurua, "Optical spectroscopy of conductive junctions in plasmonic cavities," *Nano Lett.* **10**, 3090-3095 (2010).
18. O. Pérez-González, N. Zabala, and J. Aizpurua, "Optical characterization of charge transfer (CTP) and bonding dimer (BDP) plasmons in linked interparticle gaps," *New J. Phys.* **13**, 083013 (2011).
19. R. Esteban, A.G. Borisov, P. Nordlander and J. Aizpurua, "Bridging quantum and classical plasmonics with a quantum-corrected model," *Nature Communications* **3**, 825 (2012).
20. D.C. Marinica, A. K. Kazansky, P. Nordlander, J. Aizpurua, and A. G. Borisov, "Quantum plasmonics: nonlinear effects in the field enhancement of a plasmonic nanoparticle dimer," *Nano Lett.* **12**, 1333–1339 (2012).
21. K. J. Savage, M. M. Hawkeye, R. Esteban, A.G. Borisov, J. Aizpurua, and J.J. Baumberg, "Revealing the quantum regime in tunnelling plasmonics," *Nature* **491**, 574–577 (2012).
22. J.A. Scholl, A. García-Etxarri, A. L. Koh and J.A. Dionne, "Observation of quantum tunneling between two plasmonic nanoparticles," *Nano Lett.* **13** (2), 564-569 (2013).
23. L. Venkataraman, J. E. Klare, I. W. Tam, C. Nuckolls, M. S. Hybertsen, and M. L. Steigerwald, "Single-molecule circuits with well-defined molecular conductance," *Nano Lett.* **6**, 458–462, (2006).
24. J. Bellesa, C. Bonnand, J.C. Plenet, and J. Mugnier, "Strong coupling between surface plasmons and excitons in an organic semiconductor," *Phys. Rev. Lett.* **93**, 036404 (2004).
25. G.A. Wurtz, P.R. Evans, W. Hendren, R. Atkinson, W. Dyckson, R.J. Pollard, and A. V. Zayats, "Molecular plasmonics with tunable exciton-plasmon coupling strength in J-aggregate hybridized Au nanorod assemblies," *Nano Lett.* **7**, 1297–1303 (2007).
26. N.T. Fofang, T. Park, O. Neumann, N.A. Mirin, P. Nordlander and N.J. Halas, "Plexciton nanoparticles: plasmon-exciton coupling in nanoshell-J-aggregates complexes," *Nano Lett.* **8**, 3481-3487 (2008).
27. D. E. Gómez, K. C. Vernon, P. Mulvaney, and T. J. Davis, "Surface plasmon mediated strong exciton-photon coupling in semiconductor nanocrystals," *Nano Lett.* **10**, 274–278 (2010).
28. M. Geiser, F. Castellano, G. Scalari, M. Beck, L. Nevou, and J. Faist, "Ultrastrong coupling regime and plasmon polaritons in parabolic semiconductor quantum wells," *Phys. Rev. Lett.* **108**, 106402 (2012).
29. A. Manjavacas, F.J. García de Abajo, and P. Nordlander, "Quantum plexcitonics: strongly interacting plasmons and excitons," *Nano Lett.* **11**, 2318–2323 (2011).
30. L. J. Sherry, S. H. Chang, G. C. Schatz, and R. P. Van Duyne, "Localized surface plasmon resonance spectroscopy of single silver nanocubes," *Nano Lett.* **5**, 2034–2038 (2005).
31. A. J. Haes and R. P. Van Duyne, "A nanoscale optical biosensor: sensitivity and selectivity of an approach based on the localized surface plasmon resonance spectroscopy of triangular silver nanoparticles," *J. Am. Chem. Soc.* **124**, 10596–10604 (2002).
32. J.M. Nam, C. S. Thaxton, and C. A. Mirkin, "Nanoparticle-based bio-bar codes for the ultrasensitive detection of proteins," *Science* **301**, 1884–1886 (2003).
33. E. Galopin, J. Niedziółka-Jönsson, A. Akjouj, Y. Pennec, B. Djafari-Rouhani, A. Noul, R. Boukherroub, and S. Szunerits, "Sensitivity of plasmonic nanostructures coated with thin oxide films for refractive index sensing: experimental and theoretical investigations," *J. Phys. Chem. C*, **114** 11769–11775 (2010).
34. F. López-Tejiera, R. Paniagua-Domínguez and J. Sánchez-Gil, "High-performance nanosensors based on plasmonic Fano-like interference: probing refractive index with individual nanorice and nanobelts," *ACS Nano* **6**, 8989-8996 (2012).
35. F.J. García de Abajo and A. Howie, "Retarded field calculation of electron energy loss in inhomogeneous dielectrics," *Phys. Rev. B* **65**, 115418 (2002).
36. P.B. Johnson and R. W. Christy, "Optical constants of the noble metals," *Phys. Rev. B* **6**, 4370 (1972).
37. M. Dressel and G. Grüner, *Electrodynamics of solids* (Cambridge University Press, U.K., 2002).
38. K.E. Oughstun and N.A. Cartwright, "On the Lorentz-Lorentz formula and the Lorentz model of dielectric dispersion," *Optics Express* **11**, 1541-1546 (2003).
39. O. Pérez-González, *Optical properties and high-frequency electron transport in plasmonic cavities*, PhD Thesis, (University of the Basque Country, UPV-EHU, 2011).
40. N. Zabala, O. Pérez-González, P. Nordlander, and J. Aizpurua, "Coupling of nanoparticle plasmons with molecular linkers," *Proc. of SPIE* **8096**, 80961L (2011).

41. J. J. Sánchez-Mondragón, N. B. Narozhny, and J. H. Eberly, "Theory of spontaneous-emission line shape in an ideal cavity," *Phys. Rev. Lett.* **51**, 550–553 (1983).
 42. G.S. Agarwal, "Vacuum-field Rabi splittings in microwave absorption by Rydberg atoms in a cavity," *Phys. Rev. Lett.* **53**, 1732–1734 (1984).
 43. S. Rudin and T.L. Reinecke, "Oscillator model for vacuum Rabi splitting in microcavities," *Phys. Rev. B* **59**, 10227–10233 (1999).
 44. X. Wu, S. K. Gray, and M. Pelton, "Quantum-dot-induced transparency in a nanoscale plasmonic resonator," *Opt. Express* **18**, 23633–23645 (2010).
-

1. Introduction

During the last decade, the study of the interaction between light and nanometer-sized metallic particles has turned into a central and multidisciplinary area of research in nanoscience [1–3]. This emerging field, called plasmonics, has been mainly boosted by the convergence of excellent computational tools and improved fabrication and optical characterization methods, which have led to extremely interesting potential applications in biosensing, surface-enhanced spectroscopies, cancer therapies, renewable energies and active devices [4–8]. A key property of metallic nanoparticles is the dependence of the energies of their Localised Surface Plasmon Resonances (LSPRs) on the geometry of the structure, as well as the sensitivity of the energy of these resonances to the dielectric environment. In order to tailor the resulting optical properties, a huge variety of nanostructures has been engineered showing different shapes, materials or geometric distributions [9–11].

Among different designs, dimers have emerged as a useful canonical nanostructure to understand many basic processes in plasmonics [12–16]. In a dimer, two nanoparticles are placed close to each other giving rise to new resonant modes which are a result of the coupling between particles [12]. For nearly touching particles, the optical response is mainly governed by a Bonding Dimer Plasmon (BDP) resonance, which arises from the hybridization of the dipolar modes of the individual nanoparticles [13, 14]. This BDP mode presents strongly localised charge densities of opposite sign and enormously enhanced local electromagnetic fields at the cavity. In contrast, when a conductive path is established between both particles of the dimer, a Charge Transfer Plasmon (CTP) mode is allowed, with current density crossing through the cavity, involving an oscillating distribution of net charge at every individual nanoparticle [13, 14, 17, 18]. In most of the studies dealing with these effects, classical electrodynamic approaches have been applied. However, recent works incorporating quantum effects have shown that special care must be taken in sub-nanometer wide gaps, because electron tunneling through the junction gives rise to redistribution and modification of optical modes [19, 20]. This regime has been recently revealed experimentally, opening up new prospects in the field of quantum plasmonics [21, 22].

On the other hand, focusing on the field of molecular electronics, single molecules with well-defined molecular conductance [23] are commonly used as interconnects in nanoelectronics and optoelectronics. Thus, we explore here the possibility of using different molecular linkers to establish conductive paths in plasmonic dimers and to understand their role in determining the optical properties of the entire molecule-plasmonic electrodes system. The interaction between plasmonic resonances and the excitonic states supported by molecules has become a problem of current interest [8, 24–28]. Excitonic resonances in molecules or quantum dots, which consist of electron-hole pairs which can be created by the absorption of photons, couple to surface plasmon resonances creating plasmon-exciton states. These mixed states, so called plexcitons, are attractive due to their potential applications for optical devices but also because of the inherent interest of their physical properties. This problem has also been studied within a quantum mechanical approach to address the coupling between a metallic nanoparticle dimer and an excitonic quantum emitter placed in the gap [29], showing that the combined emitter-

dimer structure undergoes dramatic changes when the excitation level of the emitter is tuned across the gap-plasmon resonance.

In this paper we present a theoretical study of the optical properties of a plasmonic cavity which consists of a strongly coupled nanoparticle dimer linked by a molecular junction characterized by the presence of an excitonic transition in its constituent molecules. We model the junction with a Drude-Lorentz dielectric function, which allows to tune in a simple way both the energy of the molecules and the corresponding dynamical conductance across the junction, and also to observe the consequences in the optical behaviour of the system.

One of the main interests of plasmonic nanostructures is their potential applications as sensors. Thus, structures with increasing asymmetry producing narrow spectral lines and Fano-resonances have been exploited during the last years to take advantage of the sensitivity of their plasmonic resonances to the dielectric environment [30–34]. The potential use of these systems for sensing is based on the shifts of their plasmonic resonances as the dielectric environment is changed. In this work, in addition to a study of the usual shift-based LSPR sensing, we propose an alternative concept for LSPR sensing based on the analysis of the relative intensities of the plexcitonic resonances as the dielectric function of the environment is tuned.

In order to analyse the optical response of the system, we solve Maxwells equations in the presence of inhomogeneous media using the Boundary Element Method (BEM) to obtain the electromagnetic fields and the optical extinction spectra [35]. Local dielectric functions, described in next section, are used as an input for these calculations.

2. Dimer with a molecular linker

Our system consists of a dimer formed by two gold nanoparticles of radii $R = 50$ nm separated by a gap of $d = 1$ nm between them (see Fig. 1(a)), filled with molecules modelled as a cylindrical junction of radius a with curved endings, which match perfectly the spherical surfaces of the nanoparticles. The interparticle distance d chosen for this study is longer than the critical value for quantum tunneling effects to emerge [19], but it allows for strong plasmonic resonances in the cavity, so that the effects of loading the gap are easy to trace. Nonetheless, when a specific molecule is considered, this distance is fixed by the geometry of the molecule itself. The separation of 1 nm, chosen here, is a general separation between particles that reveals the main ingredients of the Physics of our problem. We have checked that our results are also present for other separation distances, establishing very robust spectral trends that we will detail below.

The permittivity of gold nanoparticles is taken from the literature [36]. All the molecules in the linker are assumed to be identical, characterized by a single molecular transition of energy $E_{ex} = \hbar\omega_{ex}$, so that their dielectric response as a function of frequency $\epsilon_l(\omega)$ can be described by a Drude-Lorentz function as [37, 38]:

$$\epsilon_l(\omega) = 1 - \frac{f\omega_{ex}^2}{(\omega^2 - \omega_{ex}^2) + i\omega\gamma_{ex}}, \quad (1)$$

where γ_{ex} is the damping, related to the lifetime of the molecular excitation. The dimensionless magnitude f describes the reduced oscillator strength, which is related to the density of electrons N in the junction participating in the transition. Using some approximations about the distribution of molecules in the linker [38], $\epsilon_l(\omega)$ is related to microscopic parameters so that $f\omega_{ex}^2 = 4\pi Ne^2/m$ (e and m are the charge and mass of the electron, respectively).

It is possible to connect the optical response with the conductance through the junction, similarly to our previous works for pure metallic linkers [17, 18]. The conductivity of the molecules $\kappa(\omega)$ is calculated using the relationship $\kappa(\omega) = -i\omega[\epsilon_l(\omega) - 1]/4\pi$ [37]. Then, considering the particular geometry of the linker, a spherically indented cylinder (see Fig. 1(a)), the dynamical conductance $G(\omega)$ can be obtained, by means of a geometrical factor, from the real part of

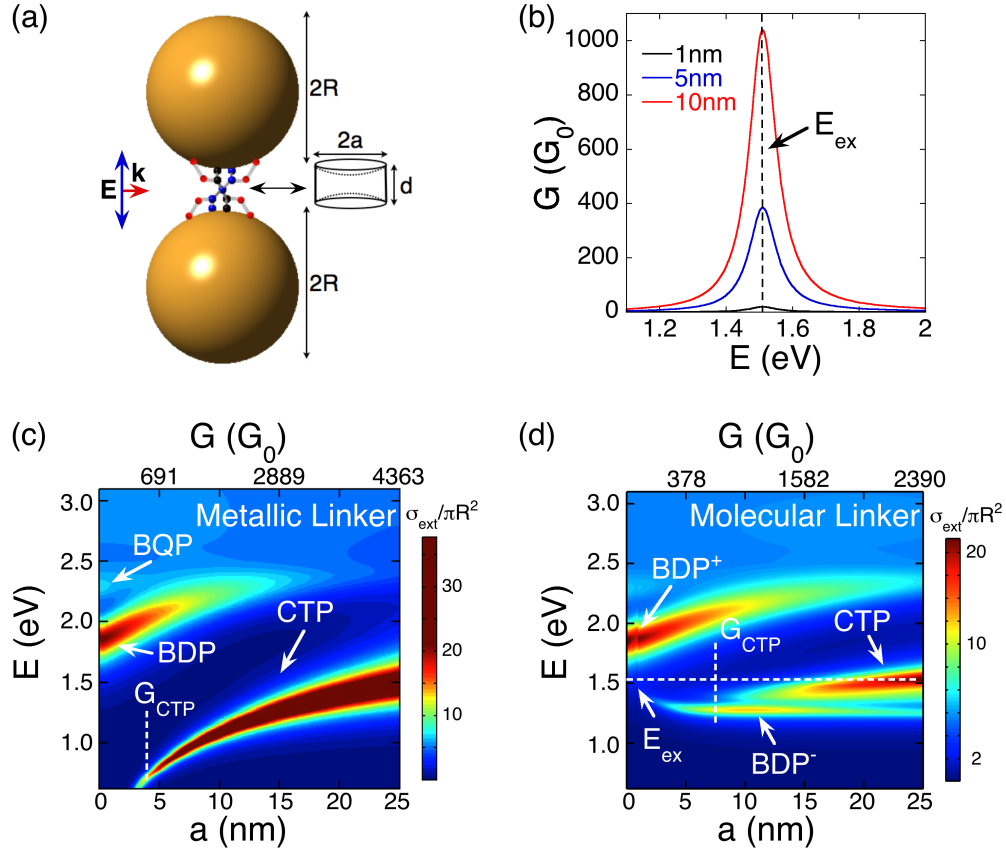


Fig. 1. (a) Schematic representation of a gold nanoparticle dimer connected by a molecular linker modelled as a cylinder of radius a and length d . The radius of the gold nanoparticles is $R = 50$ nm and the minimum separation distance between them is $d = 1$ nm (proportionality is not respected in this sketch). \mathbf{k} is the wave vector of the incident electromagnetic plane wave with polarization of the electric field \mathbf{E} along the vertical symmetry axis of the system. (b) Resonant behaviour of the conductance G for molecular linkers of radii $a = 1$ nm, 5 nm and 10 nm represented by the dielectric function of Eq. (1) with parameters $E_{ex} = \hbar\omega_{ex} = 1.51$ eV, $f = 1.5$ and $\gamma_{ex} = 0.1$ eV. (c) Calculated normalised optical extinction cross-section of a gold nanoparticle dimer bridged by a gold linker as a function of its radius a , and therefore as a function of conductance G as well. G_{CTP} is the conductance threshold of the cavity load for the emergence of the CTP mode, as given by Eq. (3). (d) Analogous calculations as in (c), but with a molecular load described by a Drude-Lorentz dielectric function using the same parameters as in (b).

the conductivity $\kappa_1(\omega)$ as follows [18,39]:

$$G(\omega) = \kappa_1(\omega)\pi\left\{\sqrt{R^2 - a^2} - R + (d/2 + R) \ln\left[1 + 2(R - \sqrt{R^2 - a^2})/d\right]\right\}. \quad (2)$$

In order to evaluate this model and explore conditions of strong plasmon-exciton interaction with large conductance, we have initially considered the excitonic energy of rotaxane

molecules, $E_{ex} = 1.51$ eV ($\lambda_{ex} = 821$ nm) [8], damping factor $\gamma_{ex} = 0.1$ eV and reduced oscillator strength $f = 1.5$. We have selected a value of f large enough for the excitation of all the possible modes to show up in the system, including the CTP mode. We have performed additional calculations for smaller values of f and we have found that wider junctions are needed to excite the CTP mode. Nevertheless, for each particular case, this parameter should be evaluated taking into account a more detailed description of the molecules, considering ab-initio values of the oscillator strength of the transitions, the density of molecules or from experimental values of the absorption.

The resonant behavior of the dynamical conductance provided by the present model is shown in Fig. 1(b), where the conductance is expressed in units of the quantum of conductance $G_0 = 2e^2/h = 7.7 \times 10^{-5}$ S (e is the electron charge and h the Planck constant). We notice that the conductance through the molecule shows a lorentzian profile with a peak centred at energy $E = E_{ex}$, and its maximum value increases when wider junctions are considered.

To analyse the optical properties of the system as a function of the radius of the linker, i.e., when increasing the number of molecules connecting the nanoparticle dimer, and thus the corresponding conductance, we calculate the optical extinction cross-section when the dimer is illuminated by light with the electric field polarized along the longitudinal axis of the linker, as sketched in Fig. 1(a). As a reference, we first review the main trends in the optical response of dimers linked by pure metallic materials in Fig. 1(c), where the results for two gold nanoparticles connected by a gold load at the gap are displayed. It is well known that the BDP and the CTP are the main modes in this case, and that there is also a transfer of spectral weight from the BDP to the CTP mode as the radius a (and so the conductance G) are increased [13, 14, 16–18]. The BDP mode, arising from the hybridization of the dipolar modes ($l = 1$) of the individual nanoparticles, is the dominant mode when the particles are disconnected, and also when narrow linkers are considered. The BDP blue-shifts towards higher energies as the linker becomes wider (the conductance of the linker is thus increased). In contrast, the CTP mode, not allowed for the empty cavity and arising from the hybridization of the monopolar modes ($l = 0$) of the nanoparticles, emerges for a given width of the molecular load, blue-shifts and eventually saturates at a given energy $E_{CTP} = \hbar\omega_{CTP}$ as the radius of the linker is increased (implying an increase of the conductance).

The conductance threshold value, which estimates the necessary conductance for the emergence of the CTP mode in conductive linkers, is found to be [17]:

$$G_{CTP} = \omega_{CTP}R^2/4\pi d. \quad (3)$$

We can observe in Fig. 1(c) that the CTP mode saturates at an energy around $E_{CTP} = 1.49$ eV ($\lambda_{CTP} = 835$ nm) for very large conductance, yielding a threshold value of $G_{CTP} \approx 656G_0$ according to Eq. (3). This G_{CTP} value, marked in the figure by a dashed, white line, fits very well the full electrodynamic calculations.

In addition to the BDP and CTP modes, a Bonding Quadrupolar Plasmon (BQP) mode is also observed as a small spectral feature around $E_{BQP} = 2.30$ eV ($\lambda_{BQP} = 540$ nm). This BQP mode, arising from the hybridization of the quadrupolar modes ($l = 2$) of the individual nanoparticles, loses intensity as the conductance of the plasmonic cavity increases [18].

We describe now the results shown in Fig. 1(d), where a molecular linker with an excitonic excitation is considered. In this case the plasmonic resonances of the cavity show a more complex optical response than in the case of the metallic load, since the plasmon-exciton coupling produces a splitting of the BDP mode, which also affects the CTP. We have checked the nature of each plasmon resonance and assigned their character by analysing the symmetry of the near-field modes calculated for each branch [40]. For the molecular linker, the BDP and BQP modes, initially found at $E_{BDP} = 1.85$ eV ($\lambda_{BDP} = 670$ nm) and $E_{BQP} = 2.30$ eV ($\lambda_{BQP} = 540$

nm), corresponding to the situation where there is no molecule in the gap, also blue-shift and lose intensity progressively as a , and thus conductance G , are increased. However, two resonant modes appear in the Near-Infrared (NIR) range of the spectrum, in contrast to the only presence of the CTP resonance in the case of the metallic linker at long wavelength region in Fig. 1(c). From the near-field maps [40], we have checked that the most red-shifted resonance, around $E \approx 1.24$ eV ($\lambda \approx 1000$ nm), also has a BDP character, exactly as the blue-shifted BDP. In contrast, the resonance around $E \approx 1.55$ eV ($\lambda \approx 800$ nm) presents a clear CTP profile. Another remarkable difference between the response of metallic (Fig. 1(c)) and molecular (Fig. 1(d)) linkers is that, for the molecular case, the CTP mode does not emerge blue-shifting from the NIR range of the spectrum, as for the metallic linker, but it appears approximately at the transition energy E_{ex} of the exciton. Consequently, these results show that a more complex description to characterize the optical response of the load strongly affects the behaviour of the plasmonic cavity modes. We have also performed additional calculations for larger values of the interparticle distance d , observing a completely analogous splitting of the modes and the same physical trends, thus establishing a robust pattern of spectral splittings in all cases.

In order to distinguish between the coupled modes of higher and lower energy, we have labelled them as BDP^+ and BDP^- (upper and lower branches of the splitting), respectively. In general, the optical response of the nanostructure is mainly governed by three resonant modes, BDP^+ , BDP^- and CTP. Nevertheless, the latter mode is not always present. When a smaller oscillator strength ($f = 0.2$) is considered in the dielectric response of the linker (Eq. (1)), it is also possible to observe the splitting of the BDP mode into two modes, but the conductance through the linker is not enough to allow the emergence of the CTP mode. In the case of the molecular linker under consideration in Fig. 1(d), the CTP mode saturates around $E_{CTP} = 1.52$ eV ($\lambda_{CTP} = 815$ nm), leading to a threshold of conductance $G_{CTP} \approx 672G_0$, as calculated from Eq. (3). This threshold value is in good agreement with the emergence of the calculated CTP mode observed in Fig. 1(d), indicating that the concept of threshold of conductance introduced for pure metallic linkers is still valid when considering linkers described by a more sophisticated response. The prediction of the emergence of the CTP mode can be very useful when different molecular linkers are present in the cavity, as we consider in next section, where the energy of the molecules is tuned across the cavity plasmon resonances.

3. Plexcitonic splitting

It is well known in the context of atomic physics that the presence of an atom or molecule produces the splitting of the resonances in an optical cavity [41–43]. Similarly, in our system, the cavity BDP and BQP plasmon resonances can couple to the excitons of the molecular linker, giving rise to mixed plasmon-exciton modes so called plexcitons [24–26]. This coupling of the plasmon modes to the excitons can be interpreted in terms of a simple model of two coupled oscillators [27, 44]. The resulting mixed BDP-exciton modes are called BDP^+ and BDP^- modes, while the mixing of the BQP to the exciton produces the BQP^+ and BQP^- modes, where + and – refer to higher and lower energies, respectively. According to this coupled-oscillator interpretation of plexcitons, their energies can be expressed as follows [27, 39, 43]:

$$E^\pm = \frac{E_P + E_{ex}}{2} \pm \left[\left(\frac{\hbar\Omega_R}{2} \right)^2 + \frac{1}{4}(E_P - E_{ex})^2 \right]^{1/2}, \quad (4)$$

where E_P and E_{ex} are the energies of the plasmonic mode (BDP or BQP) and the exciton, respectively. The term $\hbar\Omega_R$ is the Rabi splitting, which is obtained from the full electro-dynamical calculations when $E_P = E_{ex}$.

In order to explore the mixed modes in dimer cavities, we have tuned the energy of the excitonic resonance of the ensemble of molecules connecting both nanoparticles. We have changed

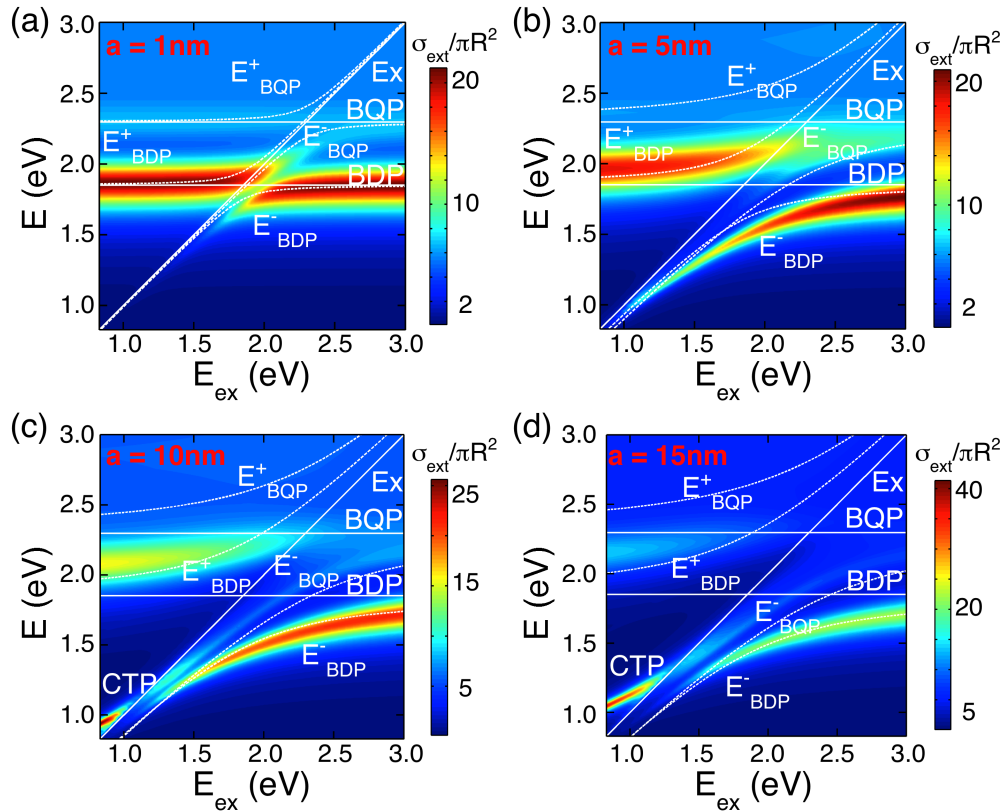


Fig. 2. Calculated normalised optical extinction cross-section of a gold nanoparticle dimer bridged by a molecular linker filling the interparticle separation of $d = 1$ nm with fixed size characterized by a molecular load radius a , as the energy and the oscillator strength of the excitonic transition in the cavity is varied. (a) $a = 1$ nm, (b) $a = 5$ nm, (c) $a = 10$ nm and (d) $a = 15$ nm. The white, solid lines included indicate the following: Ex the exciton energy line, BDP and BQP the energy lines of the dipolar and quadrupolar bonding plasmon modes when there is no linker. Finally, the white, dashed lines E_{BDP}^+ , E_{BDP}^- , E_{BQP}^+ and E_{BQP}^- indicate the energies of the coupled modes derived from Eq. (4).

the energy of the exciton E_{ex} so that the product $f\omega_{ex}^2$ in Eq. (1) is kept constant. We are thus varying at the same time the frequency ω_{ex} of the excitonic transition of the molecules and the reduced oscillator strength f describing them, while we keep constant the damping factor $\gamma_{ex} = 0.1\text{eV}$ in Eq. (1). In this manner, the conductivity and the maximum conductance for a given volume of the molecular load is fixed, i.e, the centre of the lorentzian function describing the conductance in the cavity G (see Fig. 1(b)) shifts while the intensity of its maximum does not vary.

Figure 2 shows the calculated normalised optical extinction cross-section of a gold nanoparticle dimer bridged by a molecular linker as the energy is tuned as described above, for a given material load volume (a fixed). In this case, four different radii have been considered, $a = 1$ nm, 5 nm, 10 nm and 15 nm, describing different volumes of molecular loads in the gap. Even for the thinnest linker, we observe that both the BDP and the BQP resonances split into two branches, showing an anti-crossing behaviour centred at the point of intersection of the exci-

ton energy and the BDP and BQP energy lines, indicated by white, solid lines in Fig. 2. The situation is much more evident in the case of the BDP than in the BQP due to the difference in spectral weight between both resonances (BQP is a minor spectral feature in comparison to BDP). In the splitting of the BDP mode into the BDP^- and the BDP^+ modes in Fig. 2, the energy of one of the branches, E_{BDP}^- , is below the energy of the plasmon cavity mode, while the energy of the other one, E_{BDP}^+ , is above the corresponding plasmon energy. An analogous behaviour is observed in the splitting of the BQP mode into the BQP^- and the BQP^+ modes.

Figure 2 also shows that, as the linker becomes wider (from (a) to (d), $a = 1$ nm - $a = 15$ nm), the energy splitting between the coupled modes E_{BDP}^- and E_{BDP}^+ increases. As already mentioned, the magnitude of the Rabi splitting $\hbar\Omega_R$ in Eq. (4) is estimated from the full electrodynamic simulations when $E_P = E_{ex}$ and, for the cases under consideration in this study, it is of the order of hundreds of meV. From our calculations, we have also observed that the Rabi splitting increases rapidly as the radius of the molecular load grows, but presents a saturation trend for $a > 10$ nm.

The results of the approximation derived from Eq. (4) to obtain the energy lines of the coupled modes are shown in Fig. 2 as white dashed lines superimposed to the full electrodynamic calculation (E_{BDP}^- , E_{BDP}^+ , E_{BQP}^- and E_{BQP}^+), showing a good agreement with the simulations. This agreement is slightly affected by the intense interaction between the coupled modes of the BDP and the BQP resonances, which increases as the linker becomes wider, and by the presence of the CTP mode as well. We would like to notice that this coupled oscillator model considers the coupling of each plasmon mode with the exciton individually, as if each plasmon mode was the only resonance in the cavity, whereas in practise both plasmon modes are present, and we therefore observe the interaction between the BDP^+ , BDP^- , BQP^+ , BQP^- and CTP modes.

It is also remarkable that in Figs. 2(c) and 2(d) ($a = 10$ nm and 15 nm), where big cavity loads of molecules are considered, we observe the emergence of the CTP mode, in contrast to the cases with small loads in Figs. 2(a) and 2(b) ($a = 1$ nm and 5 nm), where the CTP does not appear. This effect is again interpreted with the help of the concept of threshold of conductance G_{CTP} expressed by Eq. (3) [17, 18]. We have described how for very large conductance, the CTP mode saturates at energy $E_{CTP} = 1.52$ eV, leading to a threshold value of the conductance $G_{CTP} \approx 672 G_0$. For the small molecular loads in Figs. 2(a) and 2(b) the conductance of the linker is below the threshold value, thus, the CTP does not emerge. In contrast, for the big loads in Figs. 2(c) and 2(d), the conductance of the linker at the exciton energy is above the threshold value, $G(a = 10 \text{ nm}) \approx 1000 G_0 > G_{CTP}$ and $G(a = 15 \text{ nm}) \approx 1500 G_0 > G_{CTP}$. Consequently, in these cases the CTP mode is active.

We have performed additional calculations keeping fixed $f = 0.5$ and changing only the excitonic energy E_{ex} [39]. The plexciton splitting obtained in this way is similar to that of Fig. 2, but the CTP mode is not activated in such a case, because the conductance is smaller for the same load volume and the conductance threshold value is not reached at the range of energies considered. The concept of conductance threshold is thus a very useful tool to identify and predict the emergence of the CTP mode and, therefore, to analyse high-frequency transport in coupled cavities filled with optically active molecules.

4. Plexcitonic sensing

Let us explore now the sensing capabilities of the plexcitonic resonances studied above. Fig. 3 shows the calculated normalised optical extinction cross-section of a gold nanoparticle dimer with a gap between the particles of distance $d = 1$ nm, as the dielectric function of the embedding medium ϵ_d is modified. In Fig. 3(a) we consider, as a reference, the dimer with no load in the gap, while in Fig. 3(b) the particles are bridged by a molecular linker of radius $a = 3$ nm, characterized by an excitonic transition with energy $E_{ex} = 1.24$ eV, corresponding to $\lambda_{ex} = 1000$

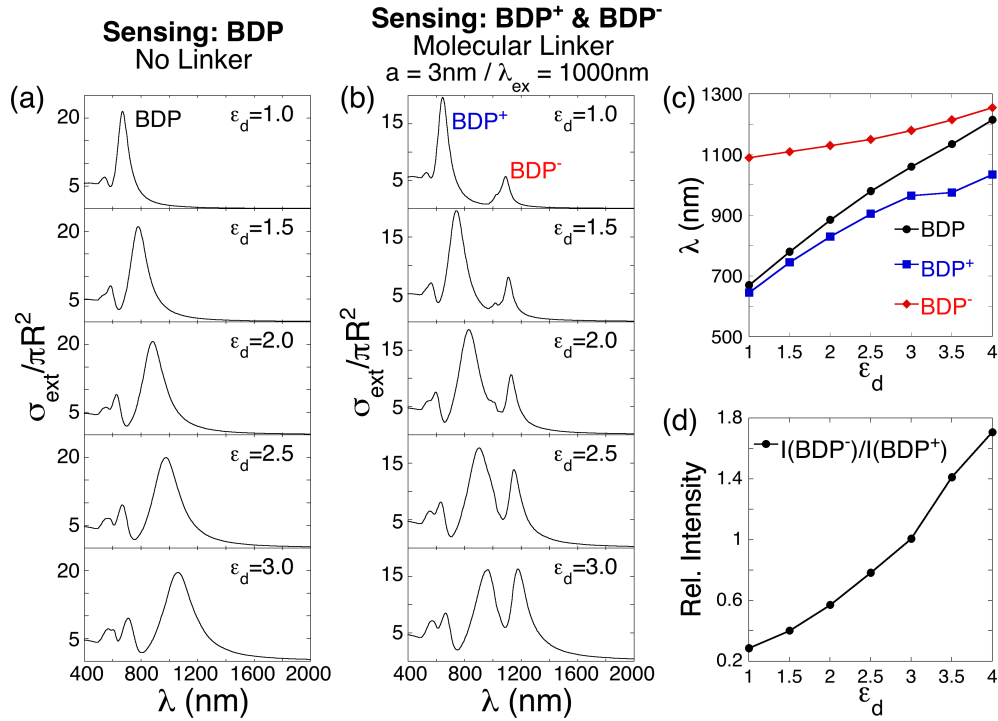


Fig. 3. (a) Calculated normalised optical extinction cross-section of a gold nanoparticle dimer with a minimum separation distance between the particles $d = 1$ nm, as the dielectric embedding constant ϵ_d is varied. (b) Calculated normalised optical extinction cross-section of a gold nanoparticle dimer bridged by a molecular linker with length $d = 1$ nm, load radius $a = 3$ nm and excitation energy $E_{\text{ex}} = 1.24$ eV ($\lambda_{\text{ex}} = 1000$ nm), as the dielectric embedding constant ϵ_d is varied. (c) Shift of the BDP, BDP⁺ and BDP⁻ modes in Figs. 3 (a) and (b) as a function of the dielectric constant of the embedding medium. (d) Variation of the relative intensity of the BDP⁺ and BDP⁻ modes in (b) as a function of the dielectric constant of the embedding medium.

nm. In the case of disconnected nanoparticles, the BDP mode, which is the plasmonic resonance governing the optical spectrum, red-shifts as the dielectric constant of the embedding medium is increased. The behaviour shown in Fig. 3(a) is similar to that of other nanostructures under similar conditions, and is the basis for conventional LSPR sensing [18, 30]. The BDP⁺ plexciton in Fig. 3(b) also presents a similar behaviour, red-shifting as the surrounding dielectric constant ϵ_d is increased. However, the BDP⁻ plexciton hardly red-shifts as ϵ_d is increased, indicating that this is not an adequate resonant mode for this type of sensing. This is also observed in Fig. 3(c), where we summarize the evolution of the shifts of the BDP (black), BDP⁺ (blue) and BDP⁻ (red) modes as a function of the dielectric constant of the embedding medium. The efficiency of plasmonic systems as sensors in shift-based LSPR sensing is usually estimated by its figure of merit (FOM), which is defined as [30]:

$$FOM = m(eV/RIU)/fwhm(eV). \quad (5)$$

In that expression m is the linear regression slope for the refractive index dependence, which indicates the ratio of the plasmon energy shift to the change in refractive index of the embedding

medium, and $fwhm$ is the full width at half maximum of the mode. From the results shown in Fig. 3(c) we obtain $FOM = 1.0$ for the BDP mode and $FOM = 0.8$ for the BDP^+ plexciton.

In the following, we focus our attention on the behaviour of the BDP^- mode, since this resonance shows a nonconventional behaviour. This plexciton, which is a minor spectral feature when the embedding medium is vacuum, hardly red-shifts as the surrounding dielectric constant ϵ_d is increased. However, by increasing ϵ_d the BDP^- mode becomes a spectral feature as strong as the BDP^+ mode in terms of intensity, as shown in Fig. 3(d), where the relative intensities of the BDP^+ and BDP^- modes change as the embedding dielectric constant ϵ_d is varied. This figure shows that, for large values of the dielectric constant, the BDP^- mode gains enough spectral weight to become more intense than the BDP^+ , indicating that the balance of spectral weight of both plexcitons can be inverted by means of a change in the dielectric embedding medium. We believe that this dramatic variation of the relative intensity of the lower energy plexciton mode might be the key for a new strategy for LSPR sensing based on the variation of the intensity of the peaks rather than on their shift.

This different behaviour of the BDP^+ and BDP^- plexciton modes can be understood with help of Fig. 2. The BDP^+ mode at the considered excitation energy $E_{ex} = 1.24$ eV presents a plasmon-like behaviour, thus red-shifting as the dielectric constant of the embedding medium is increased, as plasmon resonances do in standard localised plasmon sensing. In contrast, the BDP^- plexciton presents an excitonic-like character, thus keeping its energy constant as the medium is varied. This suggests that, depending on the desired purpose, plexciton modes can be tuned by means of the excitation energy E_{ex} to exhibit a more or less pronounced exciton/plasmon-like behaviour.

Finally we explore the sensing capabilities of the other important spectral feature of the plexcitonic system, the CTP mode, which is present when the conductance through the junction is above the conductance threshold G_{CTP} , as explained in the previous section. Fig. 4(a) shows the calculated normalised optical extinction cross-section of a gold nanoparticle dimer bridged by a molecular linker, of length $d = 1$ nm, load radius $a = 10$ nm and excitation energy $E_{ex} = 0.5$ eV ($\lambda_{ex} = 2480$ nm), as ϵ_d is varied. In Fig. 4(b) we observe clearly that the CTP mode in Fig. 4(a) is more red-shifted, as ϵ_d is increased, than the BDP mode. Figure 4(c) shows the shift of the CTP in Fig. 4 (a) *versus* the index of refraction of the embedding medium, n . The slope given by the linear regression is $m = 0.393$ eV/RIU and the $fwhm = 0.032$ eV. Thus the FOM parameter for the CTP of gold dimers connected by molecular linkers with $a = 10$ nm and excitation energy $E_{ex} = 0.5$ eV ($\lambda_{ex} = 2480$ nm) is $FOM = 12.4$. This large FOM for the CTP mode is mainly due to the remarkable shift which occurs when changing the dielectric constant of the embedding medium and also due to the sharpness of the peak. The largest FOM values in the literature, of the order of 10 – 20, have been achieved using Fano resonances [3]. Therefore, we consider that the prominent CTP mode is a good candidate for standard LSPR shift-based sensing.

5. Concluding remarks

In conclusion, we have studied theoretically the optical properties of a plasmonic cavity consisting of a strongly coupled metallic dimer when an ensemble of molecules, characterized by an excitonic transition, is placed in the cavity. The Bonding Dimer Plasmon (BDP) and the Bonding Quadrupolar Plasmon (BQP) resonances, arising respectively from the hybridization of the dipolar and quadrupolar modes of the individual nanoparticles, couple to the excitonic transition. As a consequence, these modes split into two coupled plasmon-exciton modes, called plexcitons. The Charge Transfer Plasmon (CTP) resonance, arising from the hybridization of the monopolar modes of the individual nanoparticles, is highly blue-shifted from its original spectral position and it depends strongly on the conductance of the molecular linker. The con-

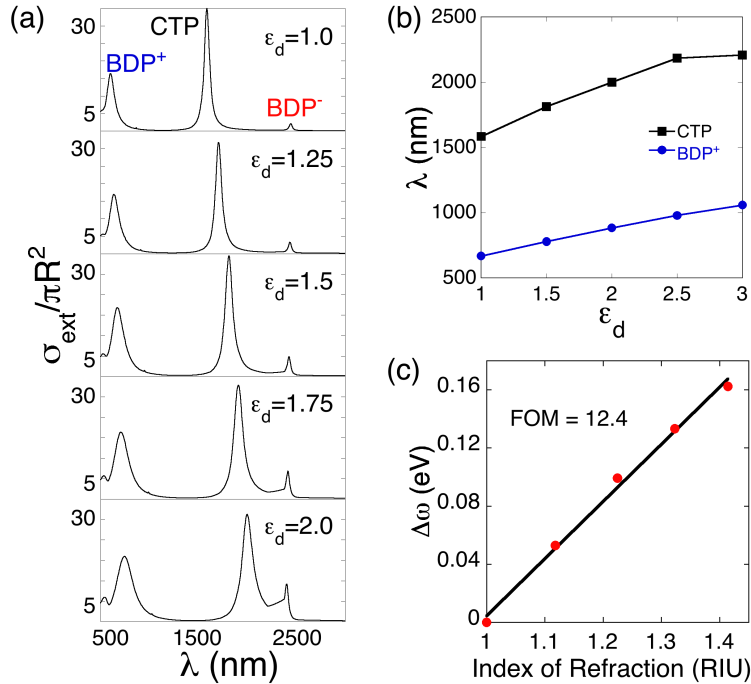


Fig. 4. (a) Calculated normalised optical extinction cross-section of a gold nanoparticle dimer bridged by a molecular linker, with length $d = 1$ nm, load radius $a = 10$ nm and excitation energy $E_{ex} = 0.5$ eV ($\lambda_{ex} = 2480$ nm), as the dielectric embedding constant ϵ_d is varied. (b) Shift of the BDP and CTP modes in Fig. 3 (a) as a function of the dielectric constant of the embedding medium. (c) Linear plot of the CTP shifts vs. refractive index of the embedding medium.

cept of conductance threshold for the emergence of the CTP mode previously introduced for metallic linkers is still valid, in spite of the complexity introduced in the linker with respect to a pure conductor.

We have explored the efficiency of the new mixed states for LSPR sensing, showing that the CTP mode is a good candidate for shift-based sensing, with a FOM value around 12. Furthermore, for the BDP-exciton mixed states, we have observed an interesting behavior for sensing based on the change of the relative intensity of the resonances, thus introducing a new framework for sensing based on the evolution of plexcitonic intensities rather than on spectral shifts.

We believe that the study of this kind of structures may contribute to improve the knowledge of plasmonic nanostructures for their use as active devices.

Acknowledgments

This project was supported by the Eortek project nanoiker from the Basque Government (BG), project FIS2010-19609-C02-01 from the Spanish Ministry of Science and Innovation and grant IT-366-07 from BG-UPV/EHU. O.P.G. acknowledges financial support from Vicerrectorado de Investigación of the University of the Basque Country (Ayudas Especialización Doctores). Computational resources were provided by DIPC (UPV/EHU, MICINN, BG, ESF).